GaN-Based High Electron-Mobility Transistors for Microwave and RF Control Applications

Nikolai V. Drozdovski and Robert H. Caverly, *Senior Member, IEEE*

***Abstract*—Heterojunction FETs or high electron-mobility transistors (HEMTs) based on $Al_xGa_{1-x}N$/GaN are studied for their use as control components for high-power microwave and RF control devices (switches, phase-shifters, etc.). A linear operation model was developed for these components so that optimum transistor geometry and operation parameters may be determined for their use in control applications. The model was verified with experimental data taken on test HEMT devices. It was experimentally established that the HEMT resistance is low for voltages of +1.0 V, and that the capacitive reactance increases for dc gate voltages below the threshold voltage of approximately −1.5 V.**

***Index Terms*—Gallium nitride, high electron-mobility transistors, microwave control.**

I. Introduction

CURRENTLY, the two most widely used microwave and RF semiconductor components for control purposes are p-i-n diodes and GaAs MESFETs. GaAs FET control devices can provide low insertion loss and high switching speed performance with minimal dc-bias power (and a minimal bias network) needed for the switching action [1]–[4]. A limitation of the GaAs FET control technology is its relatively low breakdown voltage (about 10 V). When the device is in its high impedance state, the entire RF voltage is dropped across the drain–source terminals of the transistor. Any voltage higher than the breakdown voltage will cause unwanted conduction, decreasing the isolation or possibly resulting in the destruction of the device. With such breakdown voltages, GaAs FETs are limited to power levels for individual transistors up to the range a few watts.

New semiconductor technologies based on wide-bandgap materials such as gallium nitride (GaN), because of their higher breakdown voltages, promise to extend the power level of FET-based microwave circuits by at least a factor of five [5]–[8]. A number of device structures are under development using these materials, including such structures as amplifiers and two-terminal devices [5]–[10]. These new device structures should also extend the useful power range of FET-based control components and stimulate new fully integrated high-power amplifier-control circuitry modules rather than the current hybrid and other mixed technology circuits.

Manuscript received May 11, 2000; revised December 10, 2000. This work was supported by the Office of Naval Research (J. Zolper) under Contact N000149810895.

The authors are with the Department of Electrical and Computer Engineering, Villanova University, Villanova, PA 19085 USA (e-mail: r.caverly@ieee.org).

Publisher Item Identifier S 0018-9480(02)00751-2.

While there has been significant progress made in developing GaN technology for high-power generation and amplification [5]–[10], there have been few studies to date on the use of GaN high electron-mobility transistors (HEMTs) for high-power microwave and RF control applications. In future systems based on GaN device technology, the GaN control elements will often be teamed up with high-power GaN amplifiers, thereby requiring an in-depth look at these devices in microwave and RF control environments. This paper presents the results of an in-depth investigation into modeling GaN HEMTs for small-signal applications with a look at those factors that govern high-power operation. A small-signal model is presented based on the physical and electrical properties of the device layout. This model is then compared with on-state resistance and off-state capacitance measurements that are used to both validate the model and to determine the broad-band switch cutoff frequency. The on-state resistance is then shown to be a function of the applied power levels up to +20 dBm, which is validated with experimental measurements.

II. Small-Signal Equivalent Circuit

For control applications, the source and drain connections of the HEMT are in the RF path, with the gate terminal connected to a dc voltage source that controls the state of the HEMT and, hence, the switch itself. A generalized cross section of a GaN HEMT is illustrated in Fig. 1, which shows the main network of resistances and capacitances that will be used in forming a small-signal equivalent circuit. A generally accepted figure-of-merit for comparing microwave control circuits, the broad-band cutoff frequency F_C, is defined by the on-state resistance ($R_{\rm ON}$) and off-state capacitance ($C_{\rm OFF}$) of the control element; the small-signal equivalent circuit shown in Fig. 1 defines these elements. The general expression for F_C in terms of the on-state resistance and off-state capacitance is given by

$$F_C = \frac{1}{2\pi R_{\rm ON} C_{\rm OFF}}. \tag{1}$$

The following discussion describes the model that leads to expressions that can be used to predict the on-state resistance, off-state capacitance, and the broad-band switch cutoff frequency in the GaN HEMT

The on-state resistance of the HEMT is governed by the total source–drain resistance at microwave frequencies for voltages higher than threshold. Below threshold, the two-dimensional

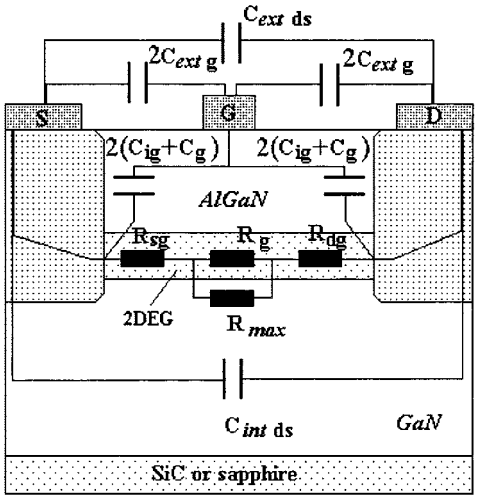

Fig. 1. Idealized HEMT structure showing the small-signal equivalent-circuit network.

electron gas (2DEG) is suppressed under the gate and the resistance increases dramatically. The general channel resistance $R_{\rm DS}$ is composed of several resistance components and may be written as

$$R_{\rm DS} = R_{\rm g} + R_{\rm sg} + R_{\rm dg} \tag{2}$$

where $R_{\rm g}$ is the interface (or channel) resistance under the gate, and $R_{\rm sg}$ and $R_{\rm dg}$ are the source–gate and drain–gate channel resistances, respectively. The contribution of $R_{\rm sg}$ and $R_{\rm dg}$ to the total on-state resistance $R_{\rm ON}$ depends on the gate–drain and gate–source electrode spacing; this spacing governs the high breakdown voltage with wider spacing yielding higher breakdown voltages [10]. The resistances making up $R_{\rm DS}$ are governed by the 2DEG that is induced at the heterointerface. Well below the threshold voltage, the 2DEG carrier density goes to zero and $R_{\rm DS}$ approaches a value $R_{\rm max}$ that is due to carriers in the GaN material. Since the 2DEG governs the resistance in the conductive channel, the resistance of each element may be estimated as

$$R_i = \rho_{\rm s} \times \frac{L_i}{W} \tag{3}$$

where $\rho_{\rm s}$ is the sheet resistance of interface channel, W is the gatewidth of HEMT, and L_i is the appropriate geometrical length. The value of the sheet resistance is dependent on the density of the 2DEG and the mobility of the carrier in the channel and can be estimated as

$$\rho_{\rm s} = \frac{1}{\mu_n n_{\rm s} q} \tag{4}$$

where q is the single charge, μ_n is the low-field mobility of 2DEG, and $n_{\rm s}$ is the 2DEG density. In estimating the resistance directly under the gate $(R_{\rm g})$, the 2DEG is assumed to be under the influence of the gate voltage, making $n_{\rm s}$ a function of the gate voltage $V_{\rm g}$. The resistance elements $R_{\rm sg}$ and $R_{\rm dg}$ are assumed to not be controlled by the applied gate voltage and, thus, $n_{\rm s}$ is not a function of $V_{\rm g}$ in the source–gate and drain–gate regions. Previous work has shown that the 2DEG density $n_{\rm s}$ may be estimated by the following expressions [11]:

$$n_{\rm s} = 2n_0 \ln\left(1 + \frac{1}{2}\exp\left(\frac{V_{\rm g} - V_T}{\eta V_{\rm th}}\right)\right) \tag{5}$$

where $V_{\rm g}$ is the dc gate voltage ($V_{\rm g}$ is zero for $R_{\rm sg}$ and $R_{\rm dg}$), η is the ideality factor, $V_{\rm th}$ is the thermal voltage for 300 K, V_T is the threshold voltage

$$n_0 = \frac{\varepsilon_i \eta V_{\rm th}}{2q(d_i + \Delta d)} \tag{6}$$

ϵ_i is the dielectric permittivity of the $Al_xGa_{1-x}N$ layer, d_i is the thickness of this layer, and Δd is the effective thickness of the 2DEG. The threshold voltage V_T is estimated from knowledge of the $Al_xGa_{1-x}N$ surface concentration n_D, barrier height ($q\Phi_B$), and conduction band discontinuity ΔE_C for the uniformly doped $Al_xGa_{1-x}N$ layer

$$V_T = \Phi_B - \frac{qn_D d_i}{2\varepsilon_i} - \frac{\Delta E_C}{q} \tag{7}$$

where n_D is the surface concentration in the $Al_xGa_{1-x}N$, $q\Phi_B$ is the barrier height between the metal gate and the $Al_xGa_{1-x}N$, and ΔE_C is the conduction-band discontinuity at the heterojunction. The value of ΔE_C was assumed to be equal to three quarters of the energy gap difference between the $Al_xGa_{1-x}N$ and GaN material. Material parameters of $Al_xGa_{1-x}N$ were determined using linear interpolation between GaN and AlN parameters as a function of the Al molar fraction x[10].

The maximum 2DEG carrier density $n_{\rm max}$ in $Al_xGa_{1-x}N$/GaN heterostructure is in the range of 1 to 2 $\times$ 10^{13} $\rm cm^{-2}$[10]. A modified 2DEG carrier density can be written as [12]

$$n_{\rm s}' = \frac{n_{\rm s}}{\left[1 + \left(\frac{n_{\rm s}}{n_{\rm max}}\right)^{\gamma_1}\right]^{1/\gamma_1}} \tag{8}$$

where γ_1 is a fitting parameter describing the saturation transition in 2DEG. Using the results of (5)–(8), the channel resistance and its gate voltage dependence may be computed using (4). According to (4) , the channel resistance decreases with n_s. For low-power operation, the low field mobility is assumed. For high-power operation, the electric field in the channel reduces the mobility, increasing the 2DEG sheet resistivity. A simple model for the high field mobility based on the geometry of the HEMT structure is used as follows:

$$\mu^{\rm high} = \frac{\mu_n}{\left(1 + \frac{\mu_n V_{sd}}{L_{\rm ch} v_{\rm sat}}\right)} \tag{9}$$

where $v_{\rm sat}$ is the saturation velocity in the 2DEG region.

Fig. 2 shows calculations using this model of $R_{\rm ON}$ in units of $\Omega\cdot$mm as a function of the 2DEG sheet resistance over the range of 1 to 1000 Ω/square. The model parameters used in this calculation are indicated in Table I. The figure shows, for example, that a 250-μm gatewidth device will exhibit an on-state resistance of 6 Ω with a sheet resistance of 500 Ω/square.

The capacitance model includes both voltage-dependent and parasitic capacitances. The voltage-dependent capacitances

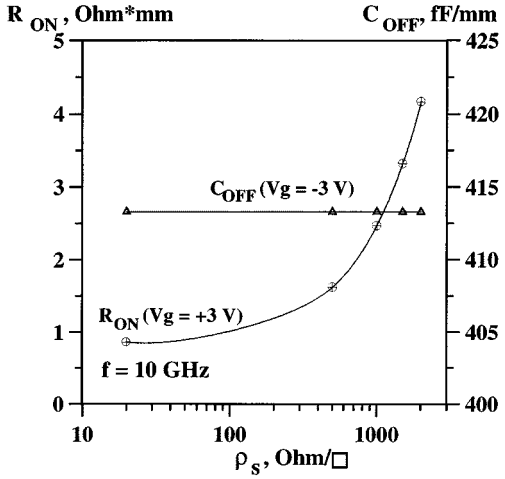

Fig. 2. On-state resistance $R_{\rm ON}$ and off-state capacitance $C_{\rm OFF}$ as a function of GaN HEMT 2DEG sheet resistance.

TABLE I
PARAMETERS FOR MODEL SIMULATION

Parameter	Value
Δd	145 Å
d_i	50 Å
γ_1, γ_3	3, 1.25
h_e	3.0 μm
gate length, L	0.3 μm
gate-drain, gate-source spacing L_i	0.85 μm
n_{max}	2 x 10^{13} cm^{-2}
μ_n	0.0545 m^2/V-s
mole fraction x	0.274

used in modeling the GaN HEMT are the source–gate and drain–gate capacitances $C_{\rm g}$, and the capacitances between the gate and inner side of the source and drain electrodes $C_{\rm ig}$. The total capacitance $C_{\rm DS}$ can be written as

$$C_{\rm DS} = C_{\rm g} + C_{\rm ig} + C_{\Sigma \rm par} \tag{10}$$

where $C_{\Sigma \rm par}$ is the total parasitic capacitance. The model described in [11] was used for the $C_{\rm g}$ calculation

$$C_{\rm g} = \frac{C_i}{1 + 2\exp\left(-\frac{V_{\rm g} - V_T}{\eta V_{\rm th}}\right)} \tag{11}$$

where C_i is the above-threshold channel capacitance

$$C_i = \frac{WL\varepsilon_i}{d_i + \Delta d}. \tag{12}$$

Taking into account the effect of the 2DEG carrier density saturation (7), a modified expression for $C_{\rm g}$ is

$$C_{\rm g}' = \frac{C_{\rm g}}{\left[1 + \left(\frac{n_{\rm s}}{n_{\rm max}}\right)^{\gamma_1}\right]^{1+1/\gamma_1}} \tag{13}$$

where γ_1 is a fitting parameter. This model describes the HEMT capacitance behavior only above the threshold voltage. When the HEMT is used as a control device, the more important capacitance is the one lower than the threshold voltage because this determines the microwave switch off-state capacitance. The off-state capacitance reflects the coupling between the gate and inner side source–drain electrodes. To estimate this capacitance, MOSFET capacitance expressions were used [13], [14] because of strong structure similarities between the HEMT and MOSFET

$$C_{\rm ig} = \frac{\varepsilon_i W}{\pi} \times \ln\left(1 + \frac{h_e}{d_i}\right) \tag{14}$$

where h_e is the depth of the electrode. When the 2DEG layer is present, this capacitance component (14) is absent, but beyond the threshold voltage V_T, $C_{\rm ig}$ plays the dominant role. This capacitance appears only after 2DEG suppression. The final approximation for this capacitance may then be written as

$$C_{\rm ig}' = C_{\rm ig}\left[1 - \left(\frac{n_{\rm s}'}{n_{\rm max}}\right)^{\gamma_3}\right]^{1/\gamma_3} \tag{15}$$

where γ_3 is a fitting parameter for the capacitance $C_{\rm ig}$. The important parasitics are (see Fig. 1) $2C_{\rm ext\ g}$, the source and drain metal coupling capacitance of the gate metal through air, the extrinsic capacitance $C_{\rm ext,ds}$ that couples the source and drain above the semiconductor, and the intrinsic capacitance $C_{\rm int,ds}$ that couples the same terminals through the semiconductor. The last two capacitances are present only in the nonconductive state, when the 2DEG is suppressed by the gate voltage. These capacitances may be estimated using a standard equation for MESFETs [4]. The off-state capacitance is independent of sheet resistance (Fig. 2).

III. Computer Simulation Results and Experimental Verification

A. Small-Signal Characterization

GaN HEMTs with 150-μm gatewidths and 0.3-μm gate lengths were used to verify the small-signal models. These test devices were designed for high-power amplifier use, but have been used here to compare the model results with experimental data for comparison purposes. The microwave and RF characteristics of the GaN HEMT under small-signal conditions were measured using a Cascade Microtech wafer-probe station connected to an HP-8510B. The measured S-parameters were converted to equivalent-circuit resistance $R_{\rm DS}$ and capacitance $C_{\rm DS}$ for comparison with the proposed model.

The resistance $R_{\rm DS}$ curves show wide variation in resistance over a 6-V tuning range. Fig. 3 compares the measured and computed switch resistance $R_{\rm DS}$ for a 0.3-μm gate-length GaN HEMT at a frequency of 2.5 GHz as a function of applied bias voltage. The resistance shows an abrupt transition in the vicinity of the threshold voltage at approximately -1.5 V. The resistance is relatively constant above about 0 V, although some improvement in resistance occurs at larger positive gate voltages as the 2DEG reaches its saturation level. Lower resistances may be obtained by either increasing the gatewidth W or increasing the 2DEG carrier density. Of the two, increasing the 2DEG carrier density is preferred since the 2DEG carrier density has minimal influence on the off-state capacitance, while increasing the

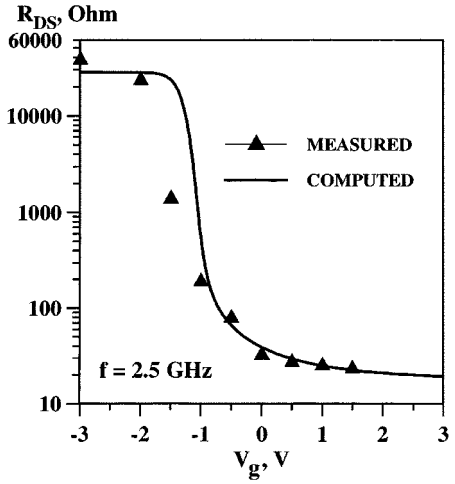

Fig. 3. Resistance $R_{\rm DS}$ versus dc gate voltage showing the resistance in the on-state (+3.0 V), off-state (−2.0 V), and in the transition region.

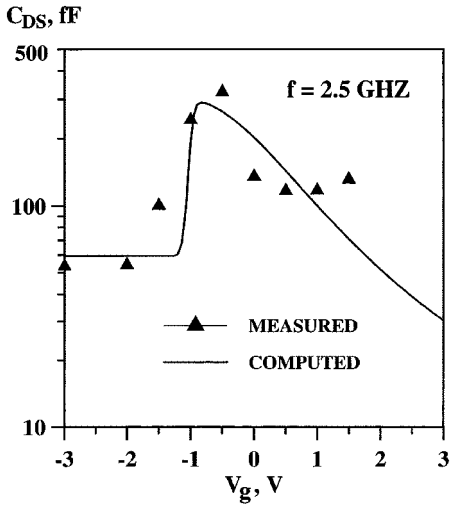

Fig. 4. Capacitance $C_{\rm DS}$ versus dc gate voltage showing the capacitance in the on-state (+3.0 V), off-state (−2.0 V), and in the transition region.

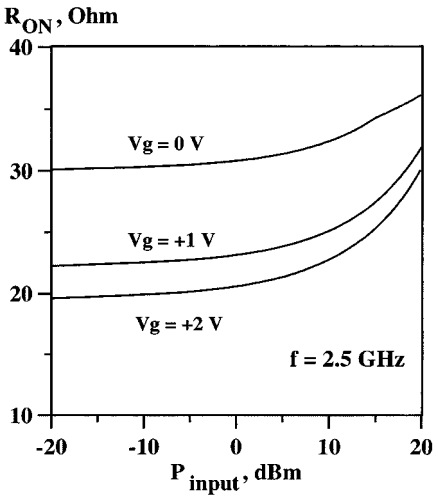

Fig. 5. The on-state resistance $R_{\rm ON}$ of the AlGaN/GaN HEMT increases above 0 dBm applied power.

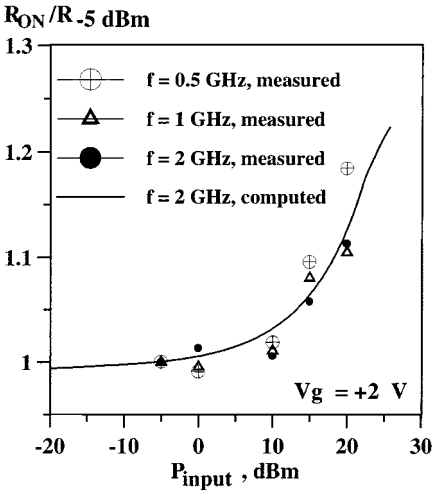

Fig. 6. Measured resistance of AlGaN/GaN HEMT control device as a function of frequency and power level, normalized to the low power (−5 dBm) value.

gatewidth will cause a corresponding increase in the off-state capacitance (Fig. 2).

The capacitance curves show constant values of capacitance at either end of the tuning range with a peak in the capacitance near the threshold voltage (Fig. 4). In the off-state (beyond V_T), the dominating switch impedance is formed by the equivalent-circuit capacitance $C_{\rm OFF}$. Note the general agreement between the capacitance at voltages above and beyond threshold in the proposed model. The small capacitances exhibited by the GaN HEMTs (less than 100 fF) indicate that these devices may be used successfully at very high frequencies. For the device with the on and off state illustrated in Figs. 3 and 4, the switch cutoff frequency is approximately 130 GHz. The peak in the capacitance in the vicinity of the threshold voltage corresponds to the operating region undergoing the most rapid change in the 2DEG carrier concentration with applied gate voltage.

B. Large-Signal Characterization

The microwave and RF resistance and capacitance of the AlGaN/GaN HEMT is a function of not only the gate–source voltage, but also the gate–drain voltage. It has been noted previously in control MESFETs [4] that drain–gate coupling of the microwave signal onto the gate electrode changes the operating point of the MESFET. This coupling also occurs in GaN HEMTs because of similar geometrical capacitances, and is a function of the microwave power level and operating frequency. The HEMT parameters influenced by this coupled signal include the increased electric field in the 2DEG, which reduces the 2DEG carrier mobility, slightly increases the 2DEG carrier density and pushes operation near the device's saturation region. Fig. 5 shows the results of simulations based on the changes in mobility and 2DEG carrier density on the on-state resistance with a power level using the gate voltage as a parameter. The simulations show on-state resistance increases dramatically with a power level above approximately 0 dBm, with about a 50% increase in resistance at 20 dBm at a gate voltage of +2.0 V.

A series of measurements of AlGaN/GaN HEMT on-state resistance versus power level were performed over the frequency

range of 0.5–8.0 GHz using the HP-8510B vector network analyzer to confirm the large-signal modeling approach. The power level across a shunt-connected GaN HEMT was varied from -5 to 20 dBm. The results of these measurements, shown in Fig. 6, indicate that the on-state resistance of the HEMT remains relatively constant up to approximately 0 dBm and then increases dramatically above 0 dBm. Only measurements up to 2.0 GHz are shown since there was little difference in resistance change above this frequency. Also shown in Fig. 6 is the simulated resistance variation (solid line) showing good agreement with measurements. It should be noted that there is a larger increase in resistance at 500 MHz than 2.0 GHz. This frequency dependence is due to the change in the operating point of the device due to added coupling of the RF voltage across the gate–source due to the corresponding gate–source and gate–drain capacitances.

IV. Conclusion

Large- and small-signal switch models have been proposed in this paper and have provided strong evidence to support the use of HEMTs based on AlGaN/GaN technology for RF, microwave, and millimeter-wave control device design. The small-signal equivalent circuit showed good agreement with low-power data taken on experimental devices. Broad-band cutoff frequencies above 100 GHz are easily achievable and will increase further as 2DEG carrier densities are increased and channel sheet resistivities decrease. The large-signal model presented accurately shows the increase in on-state resistance with an increasing power level. Further work in this area involves the investigation of the high-power performance of both the current generation of GaN HEMTs as well as newer generations based on lower surface-resistivity material.

Acknowledgment

The GaN test devices have been generously supplied by L. Eastman, Department of Electrical and Computer Engineering, Cornell University, Ithaca, NY, and B. Green, Department of Electrical and Computer Engineering, Cornell University, Ithaca, NY.

References

[1] Y. Ayalsi, "Microwave switching with GaAs FET's," *Microwave J.*, vol. 25, pp. 719–723, May 1982.
[2] A. Gopinath and J. Rankin, "GaAs FET RF switches," *IEEE Trans. Electron Devices*, vol. ED-32, pp. 1272–1278, July 1985.
[3] A. Gopinath, "Comparison of GaAs MESFET and GaAs p-i-n diodes as switch elements," *IEEE Electron Device Lett.*, vol. EDL-6, pp. 505–506, Oct. 1985.
[4] N. Jain and R. Gutmann, "Modeling and design of GaAs MESFET control devices for broad-band applications," *IEEE Trans. Microwave Theory Tech*, vol. 38, pp. 109–117, Feb. 1990.
[5] Y.-F. Wu, S. Keller, P. Kozodoy, B. P. Keller, P. Parikh, D. Kapolnek, S. P. Denbaars, and U. K. Mishra, "Bias dependent microwave performance of AlGaN/GaN MODFET's up to 100 V," *IEEE Electron Device Lett.*, vol. 18, pp. 290–292, June 1997.
[6] O. Aktas, Z. F. Fan, A. Botchkarev, S. N. Mohammad, M. Roth, T. Jenkins, L. Kehias, and H. Morkoc, "Microwave performance of AlGaN/GaN inverted MODFET's," *IEEE Electron Device Lett.*, vol. 18, no. 6, pp. 293–295, June 1997.
[7] M. A. Khan, Q. Chen, J. W. Yang, M. S. Shur, B. T. Dermott, and J. A. Higgins, "Microwave operation of GAN/AlGaN-doped channel heterostructure field effect transistors," *IEEE Electron Device Lett.*, vol. 17, pp. 325–327, July 1996.
[8] Y.-F. Wu, B. P. Keller, S. Keller, D. Kapolnek, S. P. Denbaars, and U. K. Mishra, "Measured microwave power performance of AlGaN/GaN MODFET," *IEEE Electron Device Lett.*, vol. 17, pp. 455–457, Sept. 1996.
[9] U. K. Mishra, Y-F Wu, B. P. Keller, S. Keller, and S. P. Denbaars, "GaN microwave electronics," *IEEE Trans. Microwave Theory Tech.*, vol. 46, pp. 756–761, June 1998.
[10] M. S. Shur, "GaN based transistor for high power applications," *Solid State Electron.*, vol. 42, no. 12, pp. 2131–2138, Dec. 1998.
[11] S. Sze, *Modern Semiconductor Device Physics*. New York: Wiley, 1998, ch. 2.
[12] K. Lee, M. Shur, T. Fjedly, and T. Ytterdal, *Semiconductor Devices Modeling for VLSI*. NJ: Prentice-Hall , 1993.
[13] D. Foty, *MOSFET Modeling with SPICE*. NJ: Prentice-Hall, 1997.
[14] N. Arora, *MOSFET Models for VLSI Circuit Simulation*. Berlin, Germany: Springer-Verlag, 1993.

Nikolai V. Drozdovski received the Diploma degree in electrical engineering (with honors) and the Candidate of Technical Science degree in microelectronics from the Moscow Power Engineering Institute (Technical University), Moscow, Russia, in 1983 and 1993, respectively.

He is currently with the Department of Electrical and Computer Engineering, Villanova University, Villanova, PA. He has authored or co-authored approximately 20 journal papers and 33 conference presentations. He holds ten patents. His main research interests are in RF and microwave control devices and semiconductor components such as p-i-n diodes, MESFET's, heterojunction FETs (HFETs).

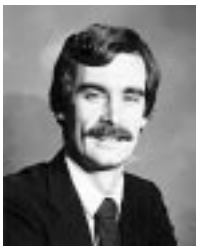

Robert H. Caverly (S'80–M'82–SM'91) received the Ph.D. degree in electrical engineering from The Johns Hopkins University, Baltimore, MD, in 1983.

He is currently a faculty member with the Department of Electrical and Computer Engineering, Villanova University, Villanova, PA. Prior to 1997, he was a faculty member with the University of Massachusetts at Dartmouth, where he began his academic career in 1983. He has authored over 50 technical articles on a variety of topics ranging from microwave control devices (primarily p-i-n diodes and MESFETs) to microwave and microelectronics education.

Dr. Caverly is an Editorial Board member for the IEEE Transactions on Microwave Theory and Techniques.